

Absorption in *p*-type Si-SiGe strained quantum-well structures

E. Corbin, K. B. Wong, and M. Jaros

Department of Physics, The University of Newcastle Upon Tyne, Newcastle Upon Tyne, United Kingdom

(Received 13 December 1993)

We present full-scale relativistic pseudopotential calculations of the first-order susceptibility in *p*-type Si-SiGe structures with a view of exploring the suitability of such systems for infrared (10–15 and 3–5 μm wavelengths) applications. The frequency dependence of the linear response due to transitions between valence minibands is calculated and the microscopic origin of the peaks determined. We also explore the effect of temperature on various structures. We show that simple particle-in-a-box models are unable to correctly describe the observed peak positions or the mechanisms involved. In particular, many important contributions come from areas of the Brillouin zone away from the zone center. We aim to show that normal incidence absorption is possible using SiGe structures.

I. INTRODUCTION

In this paper we consider the possibilities of using Si-SiGe *p*-type quantum-well structures to design infrared detectors, modulators, and switching devices. The separation of the minibands in such structures can be tuned by altering parameters such as well width, chemical composition, and the symmetry of the system. Thus the miniband structure in these systems can be modified to cover a wide range of energies and offers an opportunity to design optical devices that would operate in the mid-to-far infrared range of wavelengths. In particular, we explore the range of wavelengths of 10–15 and 3–5 μm .

The polarization angle of the incident light is of importance in the design of devices. For transitions between conduction minibands to be useful, it is necessary for the velocity vector of the incoming light to lie parallel to the growth direction. It is considerably more convenient for devices to be illuminated normal to the interface planes. We therefore consider optical effects occurring between valence minibands. In the valence band the miniband structure is complicated by the near degeneracy of the minibands at the top of the band, and by the relativistic spin-orbit effect.

In Si-SiGe systems there is also the effect of strain, caused by the lattice mismatch between the two constituents, which mixes the states characterized by the familiar bulk bands and gives rise to additional selection rules.

We shall begin with a study of absorption at 0 K in order to understand the role of the band structure in the optical sums in the simplest possible case. We predict the magnitude, the position of the main peaks in the response functions as a function of the light frequency, and identify their microscopic (band-structure) origin. We then consider the temperature dependence of both parallel and normal incidence absorption. It is hoped that a more convenient arrangement with light incident normally to the interfaces can be achieved when the excitations occur in the valence band.

II. TECHNICAL DETAILS

The initial structure studied, shown in Fig. 1, was a $\text{Si}_{0.85}\text{Ge}_{0.15}/\text{Si}$ quantum well, consisting of a 20-monolayer (27 Å) alloy well with a 40-monolayer (54 Å) Si barrier grown on a (001) Si substrate. This structure was chosen to obtain absorption in the 10–15- μm range.

The strain induced in the system due to the lattice mismatch of the alloy and barriers was considered to be confined to the alloy well, and the silicon barriers remain unstrained. A local empirical pseudopotential method was used to calculate the band structures.^{1,2} The form of the pseudopotential used was that of Freidel, Hybertsen, and Schlüter.³ In order to evaluate the susceptibility it is necessary to calculate optical sums which account for contributions coming from all points of the Brillouin zone. In our calculations only the region close to the zone center in the plane parallel to the interface contributes significantly. The sampling can be further reduced

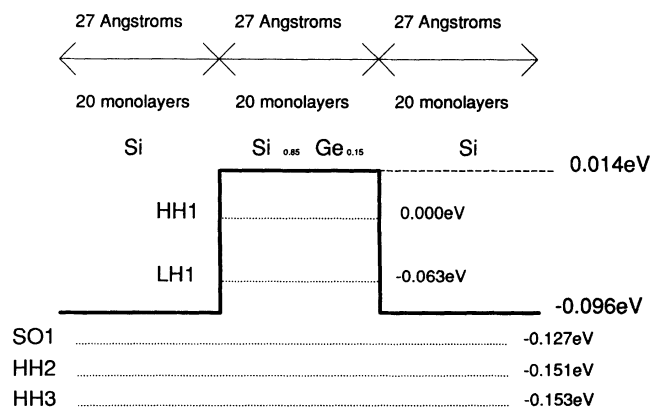


FIG. 1. Schematic representation of a $\text{Si}_{0.85}\text{Ge}_{0.15}/\text{Si}$ quantum well showing the positions of the energy levels at Γ , the zone center. The interface planes is along the z axis. The zero of energy is taken to be at the top of the superlattice valence band.

by using point-group and time-reversal symmetry, allowing the sampling to be restricted to the irreducible segment of the zone. The zero of energy was taken to be the top of the first heavy-hole (HH1) band at the zone center, Γ , and the z axis assumed to be in the growth direction. The valence-band offset was taken to be the 120 meV, from linear interpolation of the results of Van der Walle and Martin.⁴ For the first-order susceptibility, i.e., $\chi^{(1)}$ calculations only the region up to $0.2 (2\pi/a)$ (where a is the bulk lattice constant of the structure) in the x and y directions was sampled.

Both spin-orbit coupling and strain effects were considered, resulting in mixing between the valence minibands. The exchange interaction was included as a rigid shift applied to the HH1 state only, as this is the only state with significant carrier population. The magnitude of the exchange shift was estimated from the work of Bandara, Coon, and Byungsung.⁵ Other many-body

effects such as direct Coulomb interaction and correlation effects were not included at this stage.

All the results presented in this section were calculated at 0 K. The dependence of the band structure and absorption on temperature is discussed in Sec. IV. The microscopic origin of the peaks is unlikely to change with temperature, although a small shift in energy, and a broadening of the peaks may occur.

Several different "quasi" Fermi levels were used (20, 10, and 5 meV below the top of HH1 at Γ) corresponding to various doping concentrations. Park, Karunasiri and Wang⁶ state that a doping of $1 \times 10^{19} \text{ cm}^{-3}$ gives a Fermi level of -20 meV . At the Fermi levels considered, only the HH1 miniband is above the Fermi level, and hence only this band is capable of supplying carriers for transitions at 0 K.

The linear susceptibility of the system, $\chi^{(1)}$, was calculated using the formula

$$\chi_{\mu\sigma}^{(1)}(-\omega_\sigma; \omega_1) = -\frac{e^2 N}{V m \epsilon_0 \omega_\sigma \omega_1} \delta_{\mu\alpha} + \frac{e^2}{V \epsilon_0 \hbar m^2 \omega_\sigma \omega_1} \sum_k \sum_a f_a \sum_b \left[\frac{P_{ab}^\mu P_{ba}^\alpha}{\Omega_{ba} - i\Gamma_{ba} - \omega_1} + \frac{P_{ab}^\alpha P_{ba}^\mu}{\Omega_{ba} + i\Gamma_{ba} + \omega_1} \right], \quad (1)$$

where P_{ab}^μ is the optical matrix element between states a and b for incident light polarized in the μ direction, ω_1 is the frequency of the incoming beam, ω_σ is the frequency of the response, Ω_{ba} relates to the energy separation of the levels a and b , and V is the volume of the crystal. f_a is the equilibrium distribution function for electrons, which is assumed to be of Fermi-Dirac form, and Γ_{ba} is a dephasing factor which accounts for relaxation processes leading to the equilibrium distribution f_a .

The absorption of the system is given by the imaginary part of the susceptibility, i.e., $\text{Im}[\chi^{(1)}]$. The response of the quantum well can be seen to be dependent on the polarization of the incident light. Light incident parallel to the interface planes yields $\text{Im}[\chi_{zz}^{(1)}]$. The absorption when light is incident perpendicular to the plane of the interfaces is taken to be the average of $\text{Im}[\chi_{xx}^{(1)}]$ and $\text{Im}[\chi_{yy}^{(1)}]$, denoted $\text{Im}[\chi_{xx}^{(1)}]$ in the figures. By restricting the summation over indices a and b in Eq. (1), the contribution of individual processes to the total absorption can be determined.

III. 0-K RESULTS

The miniband structure along the P - Γ - X symmetry lines (i.e., from the zone edge in the growth direction to the zone center and out along the k_x axis) is shown in Fig. 2.

The minibands are labeled based on the dominant bulk-like momentum signature at Γ . Away from the zone center the mixing between valence-band states caused by the difference in the potentials of silicon and the alloy, strain and spin-orbit coupling effects mean that the bands can no longer be considered as purely heavy-hole, light-hole or spin split-off bands. No attempt has been made to smooth the band-structure diagram as that would mask the detailed features.

The diagram indicates distinct nonparabolicity of the minibands. This nonparabolicity will also contribute toward mixing between the bands. The spin split-off miniband (SO1) and the second heavy-hole miniband (HH2) can be seen to cross along the growth direction.

A. Parallel incidence

The absorption spectrum obtained when light is incident parallel to the interface planes (z polarization) and the Fermi energy is set at -20 meV can be seen in Fig. 3. The microscopic origin of the peaks, i.e., the minibands between which the transitions occur, can be seen.

Simple models suggest that the spectrum should be dominated by the HH2-HH1 transition occurring at energies around that of the zone-center separation of 151

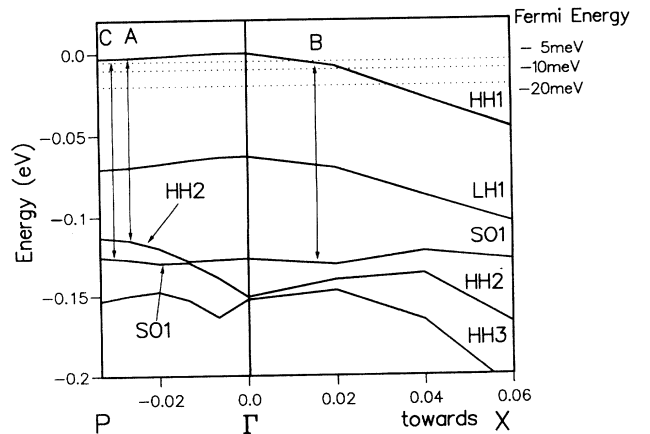


FIG. 2. Miniband structures of the $\text{Si}_{0.85}\text{Ge}_{0.15}/\text{Si}$ quantum-well structure, with a well width of 20 monolayers, along the P - Γ - X symmetry lines. See text for explanation of notes.

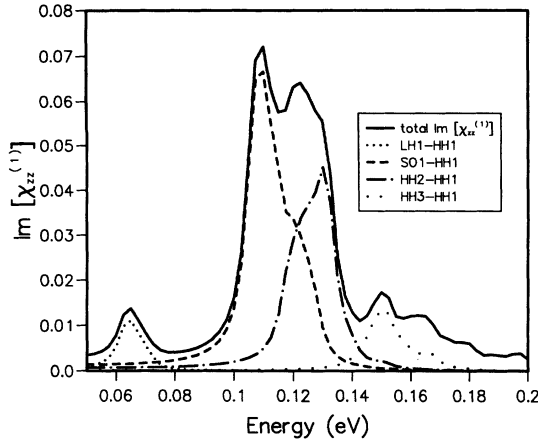


FIG. 3. Microscopic origin of absorption spectrum obtained for light incident parallel to interface planes with a Fermi energy of -20 meV for the $\text{Si}_{0.85}\text{Ge}_{0.15}/\text{Si}$ quantum-well structure, with a well width of 20 monolayers.

meV. The response is dominated, however, by a peak at ≈ 120 MeV ($\approx 11 \mu\text{m}$). It appears that much of this peak is due to a transition between SO1 and HH1. However, as indicated by arrow *A* on Fig. 2, the area of the zone in which the energy levels are ≈ 120 meV apart, the HH2 miniband is above the SO1 miniband. As the states are labeled on the basis of their nature at Γ , transitions occurring in this area of the zone are likely to be attributed to the wrong minibands. As the optical matrix elements between the two heavy-hole minibands are an order of magnitude greater than those between SO1 and HH1 in this region, it seems probable that the vast majority of the contribution to the absorption is from the HH2-HH1 transition. The HH2 state lies just outside the well for this structure, thus the dominant transition is a free-to-bound transition. Thus the expected transition dominates but the peak response occurs at an energy different from the zone-center separation of the levels.

B. Normal incidence

We now consider light incident normal to the interface planes. The variation with Fermi level of the absorption spectrum produced with normal incident light is presented in Fig. 4.

Varying the Fermi energy gives a good indication of the area of the zone in which the transition arises. The curvature of the HH1 miniband is much smaller along the growth direction than in the x - y plane. The calculations of Man and Pan⁷ indicate that states with large k_{\parallel} will be the most mixed, thus transitions which are only allowed in the presence of mixing between minibands are more likely to occur between states away from the zone center. As the Fermi level is raised to -5 meV, states with large k_{\parallel} are not available and any absorption must occur in the region round Γ and in the growth direction where the mixing of states is less pronounced.

The large peak at ≈ 125 meV is due to transitions between the SO1 and HH1 around the areas indicated by arrows *B* and *C* in Fig. 2. This transition is weakly al-

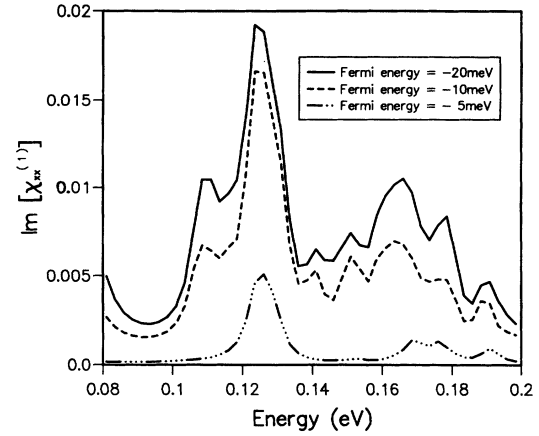


FIG. 4. Variation of the absorption spectrum with Fermi level for light incident normal to the interface planes for the $\text{Si}_{0.85}\text{Ge}_{0.15}/\text{Si}$ quantum-well structure.

lowed at Γ . Away from Γ the mixing between the SO1 and HH2 states means that the envelope function of SO1 will acquire some of the character of a HH state and hence the transition probability will be enhanced. The height of this peak drops sharply as the Fermi level is raised to -5 meV, demonstrating that much of the peak was due to transitions around *B* in Fig. 2, i.e., those with large k_{\parallel} .

Figure 5 shows the variation of absorption spectrum with polarization of the incident light. It should be remembered that although the peaks occur at similar energies, their microscopic origin is different (HH2-HH1 for parallel incidence, and SO1-HH1 for normal incidence). The height of the parallel incidence peak is about five times larger. This is because there is considerably less overlap of the envelope functions for transitions between two different valence minibands. For the parallel incidence case the transition is between two minibands with envelope functions of the same type, hence their overlap will be much larger.

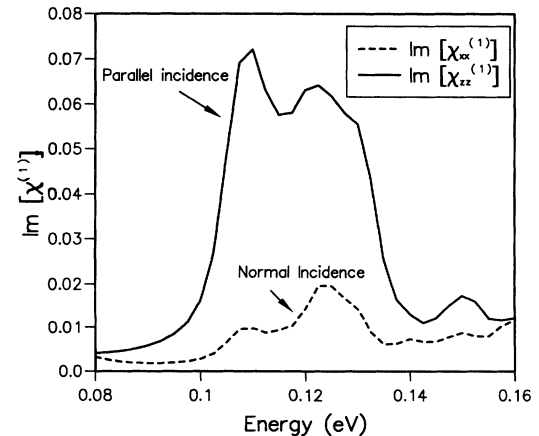


FIG. 5. Variation of absorption spectrum with the polarization angle of the incident light for the $\text{Si}_{0.85}\text{Ge}_{0.15}/\text{Si}$ quantum-well structure, with a well width of 20 monolayers.

C. Variation of response with width and composition of well

The band-structure and absorption calculations were then repeated with well widths of 28 (≈ 38 Å), 36 (≈ 49 Å), and 52 monolayers (≈ 70 Å). As the well width is increased the minibands move closer together, as would be expected from the particle-in-a-box model. In the limit of infinite well width the bulk structure should be recovered. The most notable change in the band structure as the well width is increased is that the order of the bands changes. The SO bands move more slowly and are overtaken by the light- and heavy-hole bands. This is because of the difference in the effective masses of the holes in different bands. The change in the response as well width is increased is presented in Fig. 6 for light incident parallel to the plane of the interfaces. The large peaks are all due to HH2-HH1 transitions. We can see that the peak response follows the expected trend, moving to lower energy as the well width is increased and the separation of the minibands decreases. As the well width increases more states become confined in the well, in particular the HH2 miniband moves into the well. Hence the dominant transition sequence becomes a bound-to-bound transition and thus the magnitude of the absorption increases.

The germanium concentration was then increased to 30%, and the well width varied over the same range as before. The absorption spectra produced are presented in Fig. 7. The peak response again arises from transitions between the HH2 and HH1 minibands. The response again shows the expected trend with well width and magnitude increases as degree of confinement of the HH2 band is enhanced. These results agree well with those of Fromherz *et al.*⁸ both in linewidth and energy of the peaks.

The results of varying well width for the two germanium concentrations are summarized in Fig. 8. In addition, the separation of the HH2 and HH1 levels at Γ for each structure are shown. It can be seen that the zone-center separation follows the general trend of the peak positions

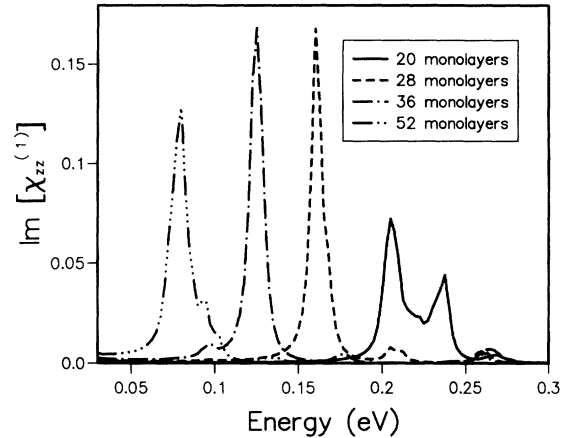


FIG. 7. Variation of the absorption spectrum with well width for light incident parallel to the interface planes for the $\text{Si}_{0.70}\text{Ge}_{0.30}/\text{Si}$ quantum-well structure. All large peaks are due to transitions between the HH2 and HH1 minibands.

but is offset slightly. This difference between the curves is most pronounced at narrower well widths. Thus a calculation performed only at Γ is unlikely to give a good representation of the structure.

Returning to the case of normal incidence, Fig. 9 shows the variation with Fermi energy of the absorption spectrum of a 28-monolayer well containing 30% germanium illuminated with light incident normal to the interface planes. The miniband dispersion along the P - Γ - X direction for this structure is shown in Fig. 10.

The intensity of the absorption is significantly less than that obtained with parallel incident light, but this structure could still be of some relevance. The large peak at $3.75\ \mu\text{m}$ is due to a bound to free transition between the LH2 and HH1 bands. The peak again decreases rapidly with decreasing Fermi levels, suggesting that the transition again occurs away from the zone center.

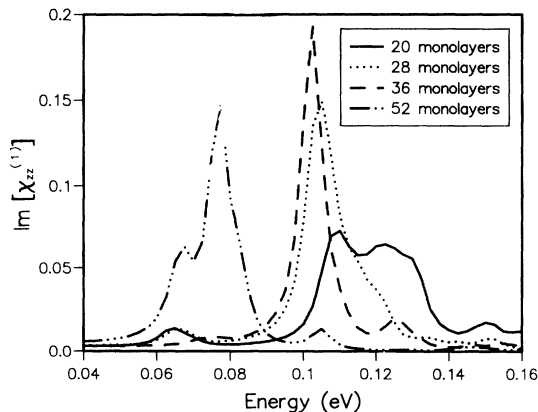


FIG. 6. Variation of the absorption spectrum with well width for light incident parallel to the interface planes for the $\text{Si}_{0.85}\text{Ge}_{0.15}/\text{Si}$ quantum-well structure. All large peaks are due to transitions between the HH2 and HH1 minibands.

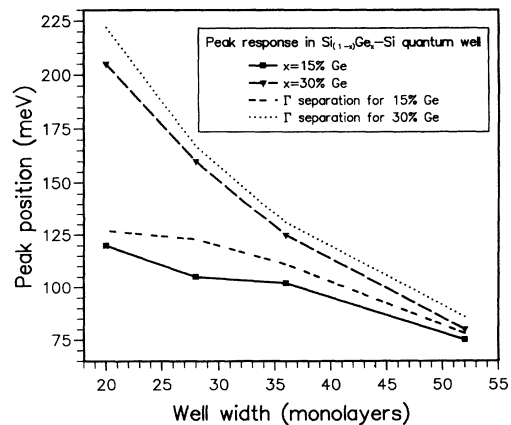


FIG. 8. Variation of the HH2-HH1 peak positions with well width for 15% and 30% germanium concentrations. The separation of the HH1 and HH2 states at Γ is also shown.

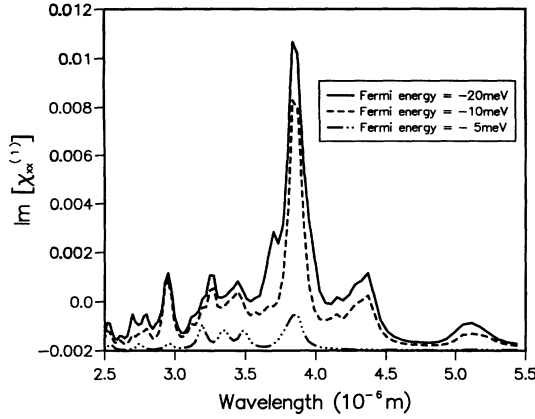


FIG. 9. Variation of the absorption with Fermi energy of a 28-monolayer well containing 30% germanium illuminated with light incident normal to the interface planes.

IV. TEMPERATURE DEPENDENCE

A. Fermi levels

Before considering the temperature dependence, we must look at the Fermi energies more closely, so that the populations of the valence minibands can be determined. To calculate the Fermi levels we use a simple effective-mass model of the quantum well, assuming that the system can be represented as a two-dimensional system with parabolic bands. It was also assumed that all the acceptors will be fully ionized, but that no electrons will have sufficient energy to be excited into the conduction band, i.e., the number of carriers within the well remains fixed. We considered 30 Å of the Si barriers to be doped to a concentration of $1 \times 10^{19} \text{ cm}^{-3}$ which gives a doping concentration per unit area of $3 \times 10^{16} \text{ cm}^{-2}$. It is further assumed that the doping concentration per unit area in the well is the same as that in the barrier. The position of the Fermi level is a function of the doping concentration, effective mass, and temperature.

The effective mass is obtained from linear interpolation of the standard values (0.49 m_0 for Si and 0.28 m_0 for

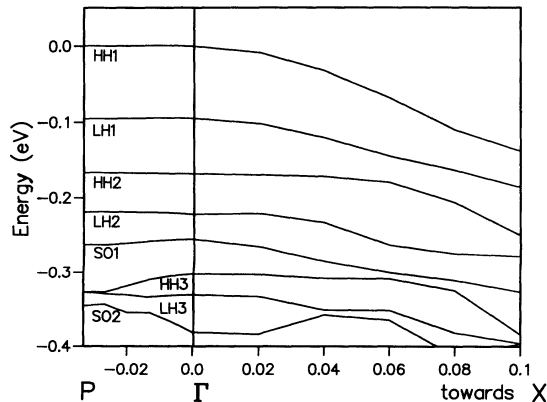


FIG. 10. Miniband structures of the 28-monolayer well containing 30% germanium along the *P*- Γ -*X* symmetry lines.

Ge). The Fermi energies calculated for different temperatures are presented in Table I.

The distribution of holes for the case of finite temperature was modeled using Fermi-Dirac statistics, including the Fermi levels calculated as above.

The susceptibility calculations were repeated for a range of temperatures between 0 K and room temperature. The band-structure calculations were not repeated for each temperature as this would be prohibitively time consuming. However, the main effect of temperature on the band structure is to alter the relative positions of the conduction and valence bands. The miniband separation within the valence band is unlikely to be altered greatly by raising the temperature. We can see from Table I that as the temperature rises the Fermi level moves toward and, at room temperature, beyond the top of the valence band at the zone center. As the temperature increases the carriers are no longer confined within the Fermi sphere and move away from the zone center to occupy states with large k_{\parallel} in the *x*-*y* plane. These are likely to be the most mixed states, and thus transition probabilities between different minibands are likely to be enhanced.

B. Parallel incidence

The temperature dependence of the structure studied in Secs. III A and III B is shown in Fig. 11. We can see that the magnitude of the peak at 110 meV, nominally attributed to the SO1-HH1 transition, rises gradually with temperature. The situation is complicated by the crossing of the minibands in the growth direction and the close proximity of the SO1 and HH1 minibands in certain areas of the zone. This makes it difficult to attribute any particular peak to a specific transition. As the temperature rises and the carriers move away from the zone center, the magnitude of the SO1-HH1 peak should increase, while that due to HH2-HH1 reduces as the proportion of carriers at the zone center decreases. The peak at approximately 110 meV, which is approximately the separation of SO1 and HH1 minibands in the *x*-*y* plane, does increase in magnitude when the temperature rises and carriers move into regions where the SO1-HH1 transition strength is greater. Thus the proportion of this peak due to SO1-HH1 increases at the expense of that due to HH2-HH1. Any more detailed behavior is masked by the general broadening of the peak at higher temperatures. The increase in width of the spectral peaks

TABLE I. Fermi energies calculated for various temperatures and germanium concentrations. The zero of energy is the top of the valence band at Γ .

Temperature	Ge concentration	
	15%	30%
0 K	-16 meV	-17 meV
77 K	-15 meV	-16 meV
150 K	-11 meV	-13 meV
225 K	-4 meV	-6 meV
298 K	+5 meV	+2 meV

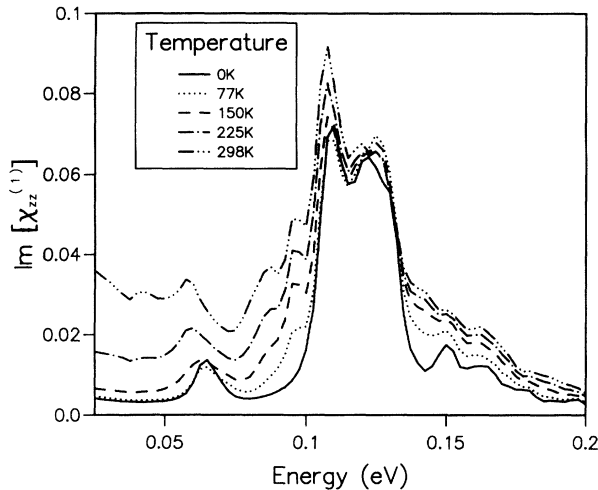


FIG. 11. Variation of the absorption spectrum with temperature for the $\text{Si}_{0.85}\text{Ge}_{0.15}/\text{Si}$ quantum-well structure with a well width of 20 monolayers, for light incident parallel to the interface planes.

is because the carriers occupy a higher proportion of the zone as the temperature increases, and thus the bandwidth of the transitions increases due to changing separation of the relevant minibands across the zone.

In Fig. 12 we can see the change of the absorption spectra with temperature for a system with a simpler band structure, the 28-monolayer, 30% germanium well. The miniband dispersion for this structure is shown in Fig. 10. As the situation is not complicated by the crossing of the minibands in this case, the general trends are easier to see. The large peak at 160 meV is a result of HH2-HH1 excitations. We can see that the magnitude of the peak decreases and the width increases as the temperature rises. There is also a corresponding increase in the small peak at 200 meV, which results from LH2-HH1 transitions. This trend can again be explained in terms of

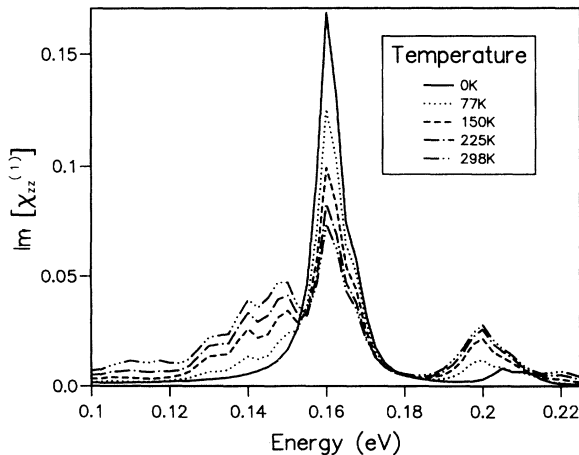


FIG. 12. Variation of the absorption spectrum with temperature for a $\text{Si}_{0.70}\text{Ge}_{0.30}/\text{Si}$ quantum-well structure with a well width of 28 monolayers for light incident parallel to the interface planes.

the carriers moving away from the center of the zone as the temperature is increased, occupying the more mixed states between which the LH2-HH1 transition probability is greater.

C. Normal incidence

For normal incidence absorption the situation is similar. For the 15% germanium structure discussed in Sec. IIIB, we can see in Fig. 13 that the normal incident response increases rapidly with temperature and the peak response moves to lower energies. Again this trend can be explained by the increased proportion of carriers occupying highly mixed states between which the probability of the SO1-HH1 transitions, which is only weakly allowed in the absence of mixing between minibands, is greatly enhanced.

We now consider the temperature dependence for normal incident absorption in the 3–5- μm range. Figure 14 shows the change in the absorption spectra as the temperature is increased for the structure consisting of a 28-monolayer well with a 30% Ge alloy as discussed in Sec. IIIC. The dominant peak at 0 K is due to the LH3-HH1 transition. As the temperature is raised and the carriers move away from the zone center, the magnitude of this peak decreases as there are less carriers available around Γ , which is where the transition probability between these two minibands is largest. The smaller peak at 200 meV is caused by LH2-HH1. This peak increases in magnitude and moves to lower energy as the temperature increases. If we look at the band structure for this system as presented in Fig. 10, we can see that the separation of the LH2 and HH1 minibands decreases along the x - y plane, explaining this energy shift. The small peak at 160 meV is a result of HH2-HH1 excitations. The magnitude of this peak again increases because of the greater transition probability between heavily mixed states.

Several areas of uncertainty remain. In particular, the inclusion of the exchange interaction as a rigid shift is ob-

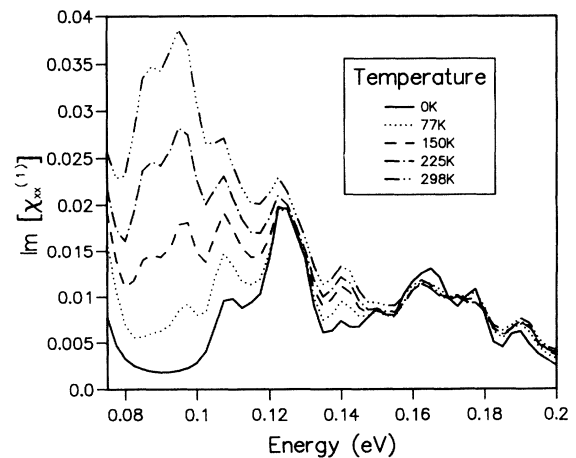


FIG. 13. Variation of the absorption spectrum with temperature for the $\text{Si}_{0.85}\text{Ge}_{0.15}/\text{Si}$ quantum-well structure, with a well width of 20 monolayers, for light incident normal to the interface planes.

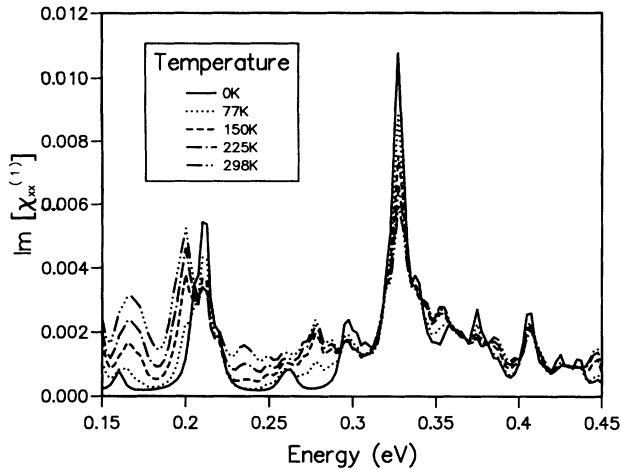


FIG. 14. Variation of the absorption spectrum with temperature for the $\text{Si}_{0.70}\text{Ge}_{0.30}/\text{Si}$ quantum-well structure, with a well width of 28 monolayers, for light incident normal to the interface planes.

viously a primitive approximation of the true situation. Other many-body effects such as the direct Coulomb interaction and the correlation or resonant screening effects have not yet been considered and may be important, particularly at high doping concentrations. There are uncertainties in the details of curvature of the valence minibands, and corresponding uncertainties with the density of states. Small changes in the potential can result in large changes in the shape of the response spectra. The

uncertainties are not in the position of the ground state but in those of the excited states, in particular the spin split-off bands. The relative position of the split-off bands is important in determining the degree of mixing between minibands and hence the strength of the normal incidence response. Thus, although the precise details of the shape of the frequency response are open to debate, the comparisons between various structures remain valid.

We have considered only ideal structures. Imperfections at the interfaces and other defects can alter the symmetry and the degree of mixing between minibands. However, we do not believe that these effects could alter our main conclusions. More work needs to be done to understand such effects quantitatively.

V. CONCLUSIONS

In conclusion, we have provided a detailed description of the processes involved in first-order susceptibility in Si-SiGe quantum-well structures. We found that for all structures considered, the linear response is dominated by transitions occurring away from the zone center. We have shown that transitions between valence minibands in Si-SiGe structures can be used to generate strong absorption with normal incident light in both the 10–15 and 3–5- μm ranges.

ACKNOWLEDGMENTS

This work was supported in part by the Defense Research Agency, Malvern and by the Office of Naval Research.

¹M. Jaros and K. B. Wong, J. Phys. C 17, L765 (1984).

²M. Jaros, K. B. Wong, and M. A. Gell, Phys. Rev. B 31, 1205 (1985).

³P. Freidel, M. S. Hybertsen, and M. Schlüter, Phys. Rev. B 39, 7974 (1988).

⁴C. G. Van de Walle and R. M. Martin, Phys. Rev. B 34, 5621 (1986).

⁵K. M. S. V. Bandara, D. D. Coon, and O. Byungsung, Appl. Phys. Lett. 53, 1931 (1988).

⁶J. S. Park, R. P. G. Karunasiri, and K. L. Wang, Appl. Phys. Lett. 60, 103 (1992).

⁷P. Man and D. S. Pan, Appl. Phys. Lett. 61, 2799 (1992).

⁸T. Fromherz, E. Koppensteiner, M. Helm, G. Bauer, J. F. Nützel, and G. Abstreiter (unpublished).